

Coverage Dependent H₂ Desorption Energy : a Quantitative Explanation Based on Encounter Desorption Mechanism

Qingkuan Meng,¹ Qiang Chang,^{1*} Gang Zhao,¹ Donghui Quan,^{2,3} Masashi Tsuge,⁴ Xia Zhang,³

Yong Zhang⁵ and Xiao-Hu Li³

¹*School of Physics and Optoelectronic Engineering, Shandong University of Technology, Zibo 255000, China*

²*Research Center for Intelligent Computing Platforms, Zhejiang Laboratory, Hangzhou 311100, China*

³*Xinjiang Astronomical Observatory, Chinese Academy of Sciences, 150 Science 1-Street, Urumqi 830011, China*

⁴*Institute of Low Temperature Science, Hokkaido University, Kita-19, Nishi-8, Kita-ku, Sapporo 060-0819, Japan*

⁵*School of Physics and Astronomy, Sun Yat-sen University, Zhuhai 519082, China*

Accepted XXX. Received YYY; in original form ZZZ

ABSTRACT

Recent experiments show that the desorption energy of H₂ on a diamond-like carbon (DLC) surface depends on the H₂ coverage of the surface. We aim to quantitatively explain the coverage dependent H₂ desorption energy measured by the experiments. We derive a math formula to calculate an effective H₂ desorption energy based on the encounter desorption mechanism. The effective H₂ desorption energy depends on two key parameters, the desorption energy of H₂ on H₂ substrate and the ratio of H₂ diffusion barrier to its desorption energy. The calculated effective H₂ desorption energy qualitatively agrees with the coverage dependent H₂ desorption energy measured by the experiments if the values of these two parameters in literature are used in the calculations. We argue that the difference between the effective H₂ desorption energy and the experimental results is due to the lacking of knowledge about these two parameters. So, we recalculate these two parameters based on experimental data. Good agreement between theoretical and experimental results can be achieved if these two updated parameters are used in the calculations.

Key words: astrochemistry – ISM: abundances – ISM: molecules

1 INTRODUCTION

Not all interstellar molecules can be efficiently formed in the gas-phase. Species such as molecular hydrogen or methanol were believed to be mainly formed on dust grains (Gould & Salpeter 1963; Watanabe & Kouchi 2002; Wakelam et al. 2017; Tsuge & Watanabe 2023). The desorption energies of surface species play essential roles in the synthesis of species on interstellar dust grains. This parameter determines the residence time of surface species on grains. Because the time period that species reside on grains must be long enough to find a partner species to react, their desorption energies must be large enough in order that these species participate in surface chemical reactions. On the other hand, because the diffusion barriers of species are believed to be proportional to their desorption energies (Hasegawa, Herbst, & Leung 1992; Herbst & van Dishoeck 2009; Garrod, Wudic Weaver, & Herbst 2008), their desorption energies must be small enough so that they can efficiently diffuse to react with other species on grain surfaces.

The desorption energies of species are usually assumed to be independent of their population on grains in astrochemical models. However, theoretical and experimental studies in the past few decades showed that the desorption energies of species are usually coverage dependent (Yates, Thiel, & Weinberg 1979; Wong et al. 2019). Moreover, the desorption energies typically decrease with the cov-

erage, which implies repulsive interactions between nearest neighbors (Wong et al. 2019). While most of these studies are not relevant to the field of astrochemistry, Tsuge et al. (2019) recently studied the coverage dependent desorption energy of H₂ on a diamond-like carbon surface, which may be analogous to interstellar dusts. They found that the H₂ desorption energy drops as the coverage of surface H₂ increases. However, Tsuge et al. (2019) did not explain the reason for their findings.

To the best of our knowledge, the coverage dependent H₂ desorption energy has not been adopted in astrochemical models, although recent studies suggest that the existence of surface H₂ should decrease H₂ desorption energy on icy grain surfaces (Hincelin, Chang, & Herbst 2015; Garrod & Pauly 2011). If we only use the desorption energy of H₂ on water ice in chemical models, almost all gas-phase H₂ molecules would be frozen on grain surfaces if the grain temperature is low (~ 10 K) and the gas number density is high ($\geq 10^{12}$ cm⁻³) (Hincelin, Chang, & Herbst 2015), which has not been observed so far. Therefore, astrochemical models usually assume a much reduced desorption of H₂ on sites already occupied by another H₂ to increase the desorption rate of surface H₂ (Hincelin, Chang, & Herbst 2015; Garrod & Pauly 2011).

A convenient way to incorporate the much reduced H₂ desorption energy on H₂ substrates in astrochemical models is to use the encounter desorption (ED) mechanism (Hincelin, Chang, & Herbst 2015; Chang et al. 2021; Zhao et al. 2022). This mechanism assumes that when a H atom or H₂ molecule encounters a H₂ molecule, its

* E-mail: changqiang@sdu.edu.cn

desorption energy immediately drops from the energy value on water ice surface to that on H₂ substrates. To include ED mechanism in rate equation models, we only have to add an reaction $\text{JH}_2 + \text{JH}_2 \rightarrow \text{JH}_2 + \text{H}_2$ or $\text{JH} + \text{JH}_2 \rightarrow \text{H} + \text{JH}_2$ in the surface reaction network, where letter J designates surface species. Rate equation chemical models that include the ED mechanism predict that the abundance of JH₂ molecules is only a few monolayers (Hincelin, Chang, & Herbst 2015), thus, these model results are not in conflict with observations.

We can use the ED mechanism to intuitively explain the coverage dependent H₂ desorption energy. As the coverage of JH₂ increases, JH₂ molecules can encounter other JH₂ molecules more frequently. So, JH₂ molecules are more likely to desorb as the population of JH₂ increases. As a result, the JH₂ desorption energy measured by experiments should decrease as the coverage of JH₂ increases.

In this work, our purpose is to quantitatively explain the coverage dependent JH₂ desorption energy. We derive a formula to calculate the coverage dependent H₂ desorption energy based on the ED mechanism and then compare with experimental results. We think that the discrepancy between our calculated coverage dependent JH₂ desorption energies and these measured by Tsuge et al. (2019) is because of the poor knowledge about two parameters, which are the diffuse barrier of JH₂ and the desorption energy of H₂ molecules when they encounter with each other. We recalculate these two parameters based on experimental data for better agreement between theoretical and experimental results.

2 METHODS

Based on the ED mechanism, JH₂ molecules desorb via two ways in the experiments performed by Tsuge et al. (2019). The first one is the thermal desorption on DLC sites while the second one is the encounter desorption of JH₂ molecules when two hydrogen molecules meet in the same site. The thermal desorption rate coefficient is,

$$k_{D1} = \nu \exp(-E_{D_{DLC}}/kT), \quad (1)$$

where $E_{D_{DLC}}$, ν , k and T are the desorption energy of JH₂ on DLC sites, the attempt frequency, the Boltzmann constant and the surface temperature respectively. In this paper, energy values are usually given in unit of K. However, if an energy value was given in unit of meV in the reference, we also express it in meV. Energy values expressed in K can be converted to that in meV by multiplying the Boltzmann constant, k . We assumed $15 \leq T \leq 25$ K because the temperature-programmed desorption (TPD) signal is too weak to be distinguished from the background noise at T that is out of the temperature range in the experiments. Tsuge et al. (2019) argued that $E_{D_{DLC}}$ should be approximately the same as the activation energy for H₂ desorption from a graphite surface (41 meV) although what they measured is well below 41 meV (476 K) at relative coverage above 0.04. Moreover, they found that the coverage dependent JH₂ desorption energy can rise as high as 40 meV (464 K) at relative coverage below 0.04. Because $E_{D_{DLC}}$ is actually the coverage dependent JH₂ desorption energy when the coverage is so low that no encounter desorption events occur on the surface, we assumed $E_{D_{DLC}} = 41$ meV (476 K) in this work. The JH₂ encounter desorption rate is (Hincelin, Chang, & Herbst 2015),

$$R_{D2} = \frac{1}{2} N_{H_2}^2 k_{enc} P_{des}, \quad (2)$$

where N_{H_2} is the population of JH₂, k_{enc} is the rate coefficient for a JH₂ molecule to encounter another one while P_{des} is the probability that JH₂ molecules desorb when the encounter events occur.

Hincelin, Chang, & Herbst (2015) found that k_{enc} can be calculated as

$$k_{enc} = \frac{2\nu}{N_s} \exp(-E_{b_{DLC}}/kT), \quad (3)$$

where N_s is the number of sites on surfaces while $E_{b_{DLC}}$ is the diffusion barrier of JH₂ on the DLC binding sites. However, the value of $E_{b_{DLC}}$ is not well known. In astrochemical models, the diffusion barrier of a species is usually chosen to be a ratio of its desorption energy. Two ratios, 0.3 or 0.5 were usually used in full gas-grain reaction network astrochemical models (Hasegawa, Herbst, & Leung 1992; Herbst & van Dishoeck 2009; Garrod, Widicus Weaver, & Herbst 2008). On the other hand, the ratio can be as high as 0.77 in the molecular hydrogen formation models (Chang, Cuppen, & Herbst 2005; Zhao et al. 2022). Therefore, we varied and studied $\alpha = E_{b_{DLC}}/E_{D_{DLC}} = 0.77, 0.5$ and 0.3 in this work. The probability P_{des} can be calculated as,

$$P_{des} = \frac{\exp(-E_{DH_2}/kT)}{\exp(-E_{DH_2}/kT) + \exp(-E_{b_{H_2}}/kT)}, \quad (4)$$

where E_{DH_2} and $E_{b_{H_2}}$ are the desorption energy and diffusion barrier of JH₂ on sites occupied by JH₂ respectively. The value of E_{DH_2} is not well known either. To the best of our knowledge, E_{DH_2} has not been measured in laboratories. So, we used two theoretical values in this work. The first one is 23 K, which was suggested by Cuppen & Herbst (2007). Based on more rigorous quantum chemical calculations, Das et al. (2021) suggested E_{DH_2} is between 67 and 79 K. So, the second value is set to be the intermediate value, 73 K as in Zhao et al. (2022). We used a scaling equation, $E_{b_{H_2}} = \alpha E_{DH_2}$ to calculate $E_{b_{H_2}}$. The total JH₂ desorption rate, R_T , is,

$$R_T = k_{D1} N_{H_2} + \frac{1}{2} N_{H_2}^2 k_{enc} P_{des}. \quad (5)$$

We assumed an effective desorption coefficient k_{eva} (Chang, Cuppen, & Herbst 2006), so that $R_T = k_{eva} N_{H_2}$. We can interpret k_{eva} as the average JH₂ desorption rate coefficient on all sites. We derived an effective desorption energy, E_{effD} by the following equation,

$$\begin{aligned} \nu \exp(-E_{effD}/kT) &= k_{eva} \\ &= k_{D1} + \frac{1}{2} N_{H_2} k_{enc} P_{des}. \end{aligned} \quad (6)$$

So, E_{effD} can be calculated as,

$$\begin{aligned} E_{effD} &= -kT \ln((k_{D1} + \frac{1}{2} N_{H_2} k_{enc} P_{des})/\nu) \\ &= -kT \ln(\exp(-E_{D_{DLC}}/kT) + \exp(-E_{b_{DLC}}/kT)\theta P_{des}), \\ &= E_{D_{DLC}} - kT \ln(1 + \exp((E_{D_{DLC}} - E_{b_{DLC}})/kT)\theta P_{des}), \end{aligned} \quad (7)$$

where θ is the relative coverage, N_{H_2}/N_s . The coverage dependent nature of E_{effD} is obvious in equation (7). Moreover, we can see that E_{effD} is a function of T , but no longer depends on ν . We will compare the derived E_{effD} with the coverage dependent H₂ desorption energy measured by Tsuge et al. (2019) in the next section.

In addition to reporting the coverage dependent H₂ desorption energy, E_{exptD} , determined using the complete analysis method (King 1975), Tsuge et al. (2019) calculated another set of coverage dependent H₂ desorption energy, E_{exptD2} based on their TPD spectrum and the Polanyi-Wigner equation. They found that E_{exptD2} agrees well with E_{exptD} . Because the variation in E_{exptD} is much larger than that in E_{exptD2} , we compare E_{effD} with E_{exptD2} in this work. If the difference between E_{effD} and E_{exptD2} is smaller than the variation in E_{exptD} , we conclude that E_{effD} agrees reasonably well with both E_{exptD2} and E_{exptD} .

In order for E_{effD} to agree better with the coverage dependent H₂ desorption energy measured in laboratories, the values of E_{DH_2} or

α may be different than these in the literature. As mentioned earlier, the values of these two parameters in the literature are no better than theoretical predictions.

If $E_{DH_{2b}}$ and α_b are the "true" values of E_{DH_2} and α , respectively, that reproduce the experimental results, they should satisfy the following equation,

$$E_{effD}(\theta, E_{DH_{2b}}, \alpha_b, T) = E_{exptD2}(\theta). \quad (8)$$

Equation (8) has two variables, $E_{DH_{2b}}$ and α_b . Because it is not possible to solve a single equation with two variables, we assumed $\alpha_b = 0.77, 0.5$ or 0.3 to calculate $E_{DH_{2b}}$. We calculated $E_{DH_{2b}}$ at five surface temperatures, 15 K, 17.5 K, 20 K, 22.5 K and 25 K. Alternatively, we assumed $E_{DH_{2b}} = 23$ or 73 K to calculate α_b at these five temperatures. Essentially, we assumed the value of one parameter (E_{DH_2} or α) in the literature is true and then calculated the other one.

We numerically solved equation (8) and calculated $E_{DH_{2b}}$ for each $E_{exptD2}(\theta)$ data point with $\alpha_b = 0.77, 0.5$ and 0.3 in the calculations. The obtained $E_{DH_{2b}}$ varies according to θ , so we calculated the average of $E_{DH_{2b}}$, $\bar{E}_{DH_{2b}}$ using the following equation,

$$\int_a^b E_{DH_{2b}}(\theta) d\theta = (b - a) \bar{E}_{DH_{2b}}, \quad (9)$$

where a and b are the minimum and maximum relative coverage respectively. We set $a = 0.03$ and $b = 0.38$ because the minimum and maximum θ in the experimental data points $E_{exptD}(\theta)$ are 0.03 and 0.38 respectively. Because $E_{DH_{2b}}$ varies according to T , the values of $\bar{E}_{DH_{2b}}$ are also different at different temperatures.

To calculate E_{effD} , we set $E_{DH_2} = \bar{E}_{DH_{2b}}$. We calculated E_{effD} using equation (7) and then compared with experimental results. We set $T = 15$ K, 20 K and 25 K in the calculations of E_{effD} . The values of E_{DH_2} were set to be the values of $\bar{E}_{DH_{2b}}$ at 15 K, 20 K and 25 K respectively in the calculations.

We also studied how well E_{effD} agree with experimental results if a temperature independent value of E_{DH_2} is used to calculate E_{effD} . Because the peak TPD signal occurs at around $T = 20$ K, we fixed E_{DH_2} to be the value of $\bar{E}_{DH_{2b}}$ at 20 K and calculated E_{effD} at $T = 15$ K and 25 K respectively. The obtained E_{effD} were also compared with experimental results.

Similarly, we set $E_{DH_{2b}} = 23$ K and 73 K respectively and solved equation (8) to calculate α_b . The average of $\alpha_b(\theta)$, $\bar{\alpha}_b$ was calculated using the following equation,

$$\int_a^b \alpha_b(\theta) d\theta = (b - a) \bar{\alpha}_b. \quad (10)$$

We set $\alpha = \bar{\alpha}_b$ and calculated E_{effD} at $T = 15$ K and 25 K respectively using equation (7). We performed two types of calculations. We set α to be the $\bar{\alpha}_b$ values at 15 K and 25 K respectively for the first one while α was fixed to be the value of $\bar{\alpha}_b$ at 20 K in the second one. The obtained E_{effD} were also compared with experimental results.

3 RESULTS

3.1 The effective H_2 desorption energy

Fig. 1 shows E_{effD} as a function of the relative coverage θ . The surface temperature is fixed at $T = 20$ K. We can see that E_{effD} qualitatively agree with E_{exptD2} and E_{exptD} regardless of the values of α or E_{DH_2} used in the calculations. The curves for $E_{effD}(\theta)$ are similar to these for $E_{exptD2}(\theta)$. The effective desorption energy is more than 464 K (40 meV) at very small relative coverage

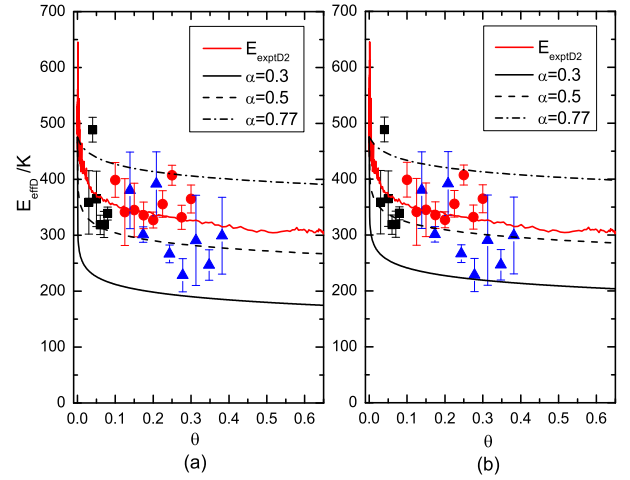


Figure 1. E_{effD} as a function of θ at fixed surface temperature $T = 20$ K. Triangles, circles and squares represent desorption energies derived by the complete analysis, E_{exptD} (Tsuge et al. 2019). Panel (a): $E_{DH_2} = 23$ K, panel (b): $E_{DH_2} = 73$ K.

($\theta \leq 0.01$). At lower coverage ($\theta < 0.04$), E_{effD} drops quickly as θ increases. But at higher coverage ($\theta > 0.04$), E_{effD} only slightly decreases as θ becomes larger.

Fig. 1 also shows that E_{effD} increases with increasing α . This phenomenon can be explained as the follows. As α increases, H_2 molecules diffuse slower on surfaces. As a result, they are less likely to encounter each other. Thus, less encounter desorption events occur as α becomes larger.

Comparing panels (a) and (b) in Fig. 1, we can see that E_{effD} also increases with increasing E_{DH_2} . This phenomenon is also easy to explain. Hydrogen molecules are less likely to desorb when they encounter with each other as E_{DH_2} becomes larger, so less desorption events occur as E_{DH_2} becomes larger.

Fig. 2 shows how surface temperatures affect E_{effD} . We fixed α and E_{DH_2} at 0.5 and 23 K respectively in the calculations. Overall, E_{effD} always increases as the surface temperature T increases. On the other hand, E_{effD} at all surface temperatures is well below E_{exptD2} .

Fig. 2 clearly shows that E_{effD} becomes larger as T becomes higher. We can analyze equation (7) to get the same conclusion. The effective desorption energy is approximately $E_D - kT \exp((E_{D_{DLC}} - E_{b_{DLC}})/kT) \theta P_{des}$ at very small θ . Because $E_D - E_b > 0$, $kT \exp((E_{D_{DLC}} - E_{b_{DLC}})/kT)$ decreases as T gets larger, thus, E_{effD} increases as T becomes larger. The dependence of E_{effD} on T is even more obvious at much larger θ . We found $E_{effD} \approx E_{b_{DLC}} - kT \ln(\theta P_{des})$ if $\exp((E_{D_{DLC}} - E_{b_{DLC}})/kT) \theta P_{des} \gg 1$. So E_{effD} linearly increases with T if θ is large enough. Therefore, our analysis shows that E_{effD} increases with increasing T at both very small and large relative coverage.

The above figures show that the discrepancy between E_{effD} and E_{exptD2} is larger than the variations in E_{exptD} . On the other hand, the similarity between curves for E_{effD} and E_{exptD} suggests that we can vary the values of α and / or E_{DH_2} in the calculations for better agreement between E_{effD} and E_{exptD2} . For instance, E_{effD} calculated using $\alpha = 0.5$ is smaller than E_{exptD2} . Because E_{effD} increases as α becomes larger, we can slightly increase E_{effD} , therefore, reduce the discrepancy between E_{effD} and E_{exptD2} by using α values that are slightly larger than 0.5 in the calculations. On

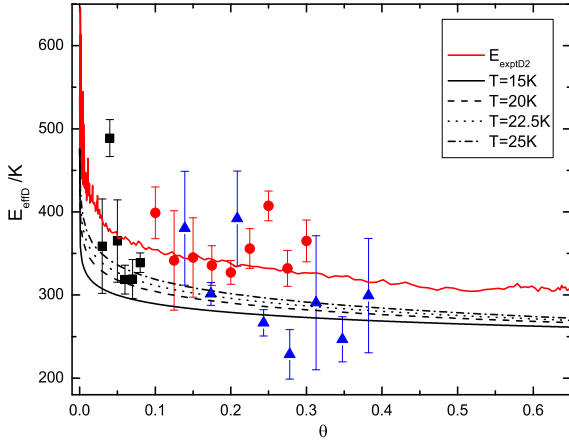


Figure 2. E_{effD} as a function of θ at various surface temperatures. $\alpha = 0.5$, $E_{DH_2} = 23$ K. Triangles, circles and squares represent desorption energies derived by the complete analysis, E_{exptD} (Tsuge et al. 2019).

Table 1. The values of $\bar{E}_{DH_{2b}}$

	$T = 15$ K	$T = 17.5$ K	$T = 20$ K	$T = 22.5$ K	$T = 25$ K
$\alpha_b = 0.3$	245 K	239 K	233 K	227 K	220 K
$\alpha_b = 0.5$	153 K	144 K	134 K	124 K	114 K

the other hand, the values of α and E_{DH_2} in the literature are just theoretical predictions. Therefore, these values may not represent the true values of α and E_{DH_2} in the experiments. So, we recalculate the values of α and E_{DH_2} based on the experimental data to reduce the discrepancy. The obtained values of these two parameters are reported in the following two subsections.

3.2 The values of $\bar{E}_{DH_{2b}}$

We assumed $\alpha_b = 0.3, 0.5$ and 0.77 to calculate $E_{DH_{2b}}$. However, we found that equation (8) does not have a solution if $\alpha_b = 0.77$ was assumed. Therefore, we only report results for $\alpha_b = 0.3$ and 0.5 in Table 1.

Table 1 shows that $\bar{E}_{DH_{2b}}$ decreases as the surface temperature becomes larger regardless of the adopted α_b values. Moreover, these $\bar{E}_{DH_{2b}}$ values are all higher than the available desorption energies of H_2 molecules on H_2 in the literature (Cuppen & Herbst 2007; Das et al. 2021). On the other hand, we can see that as α_b becomes larger, $\bar{E}_{DH_{2b}}$ becomes smaller.

We calculated $E_{effD}(\theta)$ using the $\bar{E}_{DH_{2b}}$ values listed in Table 1. The values of E_{DH_2} used in the calculations depends on the surface temperatures. Fig. 3 shows the calculated $E_{effD}(\theta)$ as a function of θ . Comparing panels (a) and (b) in Fig. 3, we found that $E_{effD}(\theta)$ agrees slightly better with experimental results if $\alpha = 0.5$ is used in the calculations. But the difference is not significant, therefore, we do not distinguish these two panels in the following discussions. At lower coverage ($\theta < 0.05$), $E_{effD}(\theta)$ is slightly smaller than $E_{exptD2}(\theta)$ for all the surface temperatures, but at higher coverage, $E_{effD}(\theta)$ is larger than E_{exptD2} . Despite the small discrepancies, the differences between $E_{effD}(\theta)$ and $E_{exptD2}(\theta)$ are less than the variations in E_{exptD} . Moreover, $E_{effD}(\theta)$ agrees better with E_{exptD2} as T increases from 15 K to 25 K. So, the newly calculated

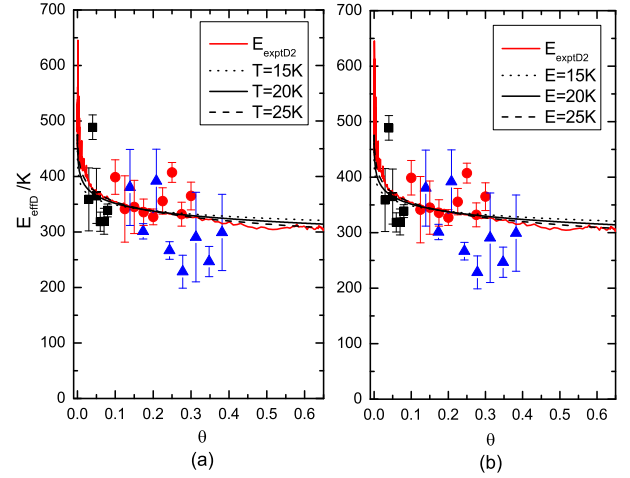


Figure 3. E_{effD} as a function of θ . The updated values of E_{DH_2} were used in the calculations, but α values are still these in the literature. The values of E_{DH_2} and α used in the calculations depend on T . Triangles, circles and squares represent desorption energies derived by the complete analysis, E_{exptD} (Tsuge et al. 2019). Panel (a): $\alpha = 0.3$, E_{DH_2} was set to be 245, 233 and 220 K for $T = 15, 20$ and 25 K respectively. Panel (b): $\alpha = 0.5$, E_{DH_2} was set to be 153, 134 and 114 K for $T = 15, 20$ and 25 K respectively.

Table 2. The values of $\bar{\alpha}_b$

	$T = 15$ K	$T = 17.5$ K	$T = 20$ K	$T = 22.5$ K	$T = 25$ K
$E_{DH_{2b}} = 23$ K	0.63	0.62	0.60	0.59	0.58
$E_{DH_{2b}} = 73$ K	0.59	0.58	0.57	0.55	0.54

$E_{effD}(\theta)$ agrees well with experimental results regardless of T and α used in the calculations.

We also calculated $E_{effD}(\theta)$ using E_{DH_2} values that are independent of T . The obtained $E_{effD}(\theta)$ is shown as a function of θ in Fig. 4. Comparing panels (a) and (b) in Fig. 4, we found that $E_{effD}(\theta)$ calculated using $\alpha = 0.3$ does not differ much from that calculated using $\alpha = 0.5$. At lower coverage ($\theta < 0.05$), $E_{effD}(\theta)$ is slightly smaller than $E_{exptD2}(\theta)$ at $T = 15$ K, however, the discrepancy between E_{effD} and E_{exptD2} almost disappears at $T = 25$ K. At higher coverage ($\theta > 0.3$), $E_{effD}(\theta)$ is always larger than $E_{exptD2}(\theta)$ regardless of T . On the other hand, the difference between $E_{effD}(\theta)$ and E_{exptD2} is also smaller than the variations in E_{exptD} . Therefore, $E_{effD}(\theta)$ calculated using the temperature independent E_{DH_2} also fits in well with the experimental results.

3.3 The values of $\bar{\alpha}_b$

Table 2 shows our calculated $\bar{\alpha}_b$ at various surface temperatures. These $\bar{\alpha}_b$ values fall within the range of α in astrochemical models ($0.3 \leq \alpha \leq 0.8$). The values of $\bar{\alpha}_b$ decreases as T becomes larger regardless of the values of $E_{DH_{2b}}$ used in the calculations. However, we can see that $(E_{DH_{2b}}(15 \text{ K}) - E_{DH_{2b}}(25 \text{ K})) / E_{DH_{2b}}(25 \text{ K}) < 0.1$, which suggests that differences of surface temperatures can only result in moderate variation of $\bar{\alpha}_b$. Finally, $\bar{\alpha}_b$ is larger if smaller $E_{DH_{2b}}$ is used in the calculations.

We set $\alpha = \bar{\alpha}_b$ and $E_{DH_2} = E_{DH_{2b}}$ to calculate E_{effD} . The values of $\bar{\alpha}_b$ depend on T . Fig. 5 shows the calculated E_{effD} as a function of θ . Comparing the two panels in Fig. 5, we found that E_{effD} calculated using $E_{DH_2} = 23$ K is almost the same as that

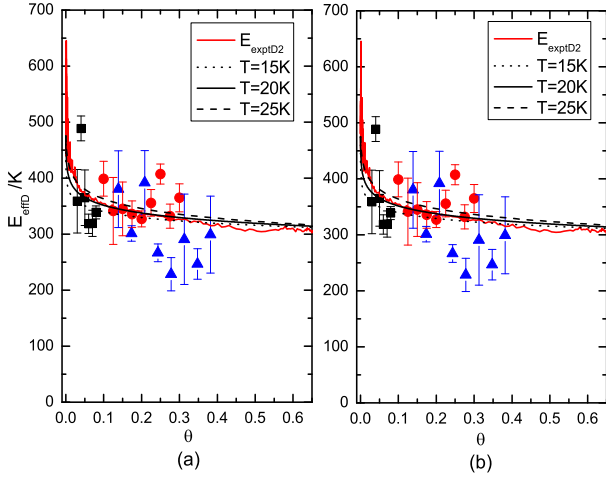


Figure 4. E_{effD} as a function of θ . The updated values of E_{DH_2} were used in the calculations, but α values are still in these in the literature. The values of E_{DH_2} and α used in the calculations do not depend on T . Triangles, circles and squares represent desorption energies derived by the complete analysis, E_{exptD} (Tsuge et al. 2019). Panel (a): $\alpha = 0.3$, $E_{DH_2} = 233$ K. Panel (b): $\alpha = 0.5$, $E_{DH_2} = 134$ K.

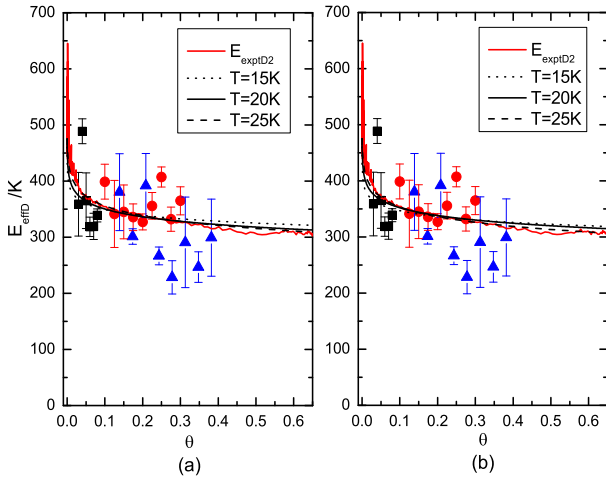


Figure 5. E_{effD} as a function of θ . The updated values of α were used in the calculations, but E_{DH_2} values used are still in these in the literature. The values of α used in the calculations depend on T . Triangles, circles and squares represent desorption energies derived by the complete analysis, E_{exptD} (Tsuge et al. 2019). Panel (a): $E_{DH_2} = 23$ K. α was set to be 0.63, 0.6 and 0.58 for $T = 15, 20$ and 25 K respectively. Panel (b): $E_{DH_2} = 73$ K. α was set to be 0.59, 0.57 and 0.54 for $T = 15, 20$ and 25 K respectively.

using $E_{DH_2} = 73$ K. At lower coverage ($\theta < 0.05$), E_{effD} is only slightly smaller than E_{exptD2} , but it becomes slightly larger than E_{exptD2} at higher coverage. The discrepancy, however, is smaller than the variations in E_{exptD} . Therefore, E_{effD} agrees well with E_{exptD} and E_{exptD2} .

Good agreement between the calculated E_{effD} and E_{exptD} (E_{exptD2}) can also be achieved as shown in Fig. 6 if temperature independent α values were used. Although E_{effD} may be slightly larger or smaller than E_{exptD2} depending on θ , the discrepancy is

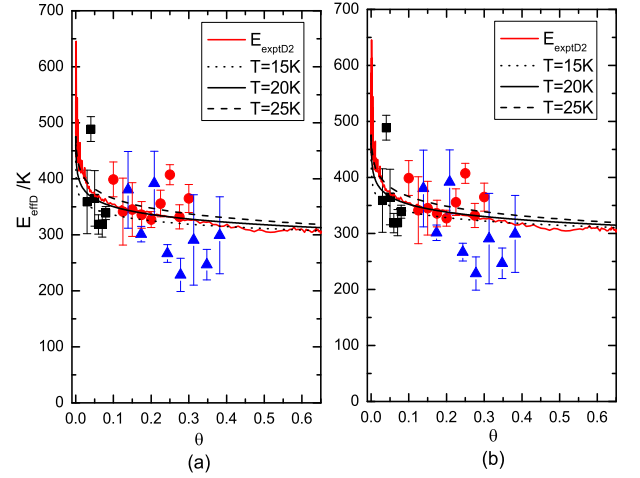


Figure 6. E_{effD} as a function of θ . The updated values of α were used in the calculations, but E_{DH_2} values used are still in these in the literature. The values of α used in the calculations do not depend on T . Triangles, circles and squares represent desorption energies derived by the complete analysis, E_{exptD} (Tsuge et al. 2019). Panel (a): $\alpha = 0.6$, $E_{DH_2} = 23$ K. Panel (b): $\alpha = 0.57$, $E_{DH_2} = 73$ K.

smaller than the variation in E_{exptD} regardless of T and the values of E_{DH_2} used in the calculations.

4 SUMMARIES AND DISCUSSIONS

Using the encounter desorption mechanism, we explained the coverage dependent H_2 desorption energy, which was experimentally measured by Tsuge et al. (2019). We suggested an effective desorption energy to compare with the coverage dependent H_2 desorption energy measured in the experiments. The value of the effective desorption energy depends on α and E_{DH_2} . Using the values of these parameters in the literature, we can only qualitatively explain the coverage dependent H_2 desorption energy measured by the experiments. We argue that the discrepancy is because of current poor knowledge about α and E_{DH_2} . So, we calculated $\bar{\alpha}_b$ and \bar{E}_{DH_2b} based on experimental data.

The values of $\bar{\alpha}_b$ and \bar{E}_{DH_2b} vary according to the surface temperatures. However, the calculated effective desorption energies at 15, 20 and 25 K agree well with experimental results even α (or E_{DH_2}) is fixed to be the value of $\bar{\alpha}_b$ (\bar{E}_{DH_2b}) at 20 K. Because the effective desorption energy increases monotonically with increasing T , all the effective desorption energies at the surface temperature range 15 - 25 K agree well with the experimental results. Because noticeable H_2 desorption occurs at temperatures between 15 K and 25 K only in the experiments (Tsuge et al. 2019), we conclude that the coverage dependent H_2 desorption energy measured by the experiments can indeed be quantitatively reproduced by our approach.

In addition to reproducing the experimental results, our approach suggested a new method to measure H_2 diffusion barriers on surfaces, which are not well known so far. Rigorous quantum chemical calculations show that $E_{DH_2} = 73$ K (Das et al. 2021) while the values of α in the literature are just crude estimations. Therefore, we argue that $E_{DH_2} = 73$ K should be close to its true value in the experiments while the values of α in the literature deviate more from its true value in the experiment. Since our calculated effective desorption energies agree well with the experimental results, we argue that $\bar{\alpha}_b$ at $T =$

20 K could be the value of α in the experiment. Therefore, the H₂ diffusion barrier on DLC surfaces prepared by Tsuge et al. (2019) could be $\bar{\alpha}_b \times 41 \text{ meV} \sim 23 \text{ meV}$ (267 K). It should be noted that that the term "DLC" represents a class of carbonaceous solid, where sp²-hybridized carbon atoms dominate. Because the α values should depend on surface, the H₂ diffusion barrier obtained above can be a representative value; it is therefore interesting to determine α values by changing the ratio of sp² and sp³ contents. In any case, this work demonstrated that the combination of laboratory experiments employing TPD and numerical simulations is a useful tool to determine α values and, therefore, the H₂ diffusion barrier for various types of surface relevant to astronomical conditions.

Finally, we comment on the validity of ED mechanism since our approach is based on it. The repulsive interaction between neighboring adsorbate molecules were believed to be the reason for the decrease of desorption energy as the coverage of adsorbates increases (Wong et al. 2019). For simplicity, we assume the repulsive interaction between adsorbate molecules is significant only when they are very close to each other, i.e., in the same binding sites. Due to the repulsive interaction, the desorption energy of adsorbates in the same binding sites should decrease, which is equivalent to reduction of desorption energy of surface species when they encounter in the ED mechanism. Therefore, the ED mechanism can be viewed as a simplification of the more complicated repulsive short-range interaction between adsorbates.

ACKNOWLEDGEMENTS

The research was funded by The National Natural Science Foundation of China under grants 12173023, 11973075, 11973099 and 12203091. We thank Eric Herbst for helpful discussions. We thank our referee for careful reading the manuscript and providing useful comments to improve the quality of the manuscript.

DATA AVAILABILITY

No new data were generated or analysed in support of this research.

REFERENCES

- Chang Q., Cuppen H. M., Herbst E., 2005, *A&A*, 434, 599.
 Chang Q., Cuppen H. M., Herbst E., 2006, *A&A*, 458, 497.
 Chang Q., Zheng X.-L., Zhang X., Quan D.-H., Lu Y., Meng Q.-K., Li X.-H., et al., 2021, *RAA*, 21, 039.
 Cuppen H. M., Herbst E., 2007, *ApJ*, 668, 294.
 Das A., Sil M., Ghosh R., Gorai P., Adak S., Samanta S., Chakrabarti S. K., 2021, *FrASS*, 8, 78.
 Garrod R. T., Wicidicus Weaver S. L., Herbst E., 2008, *ApJ*, 682, 283.
 Garrod R. T., Pauly T., 2011, *ApJ*, 735, 15.
 Gould R. J., Salpeter E. E., 1963, *ApJ*, 138, 393.
 Hasegawa T. I., Herbst E., Leung C. M., 1992, *ApJS*, 82, 167.
 Herbst E., van Dishoeck E. F., 2009, *ARA&A*, 47, 427.
 Hincelin U., Chang Q., Herbst E., 2015, *A&A*, 574, A24.
 King D. A., 1975, *SurSc*, 47, 384.
 Tsuge M., Hama T., Kimura Y., Kouchi A., Watanabe N., 2019, *ApJ*, 878, 23.
 Tsuge M., Watanabe N., 2023, *PJAB*, 99, 103.
 Wakelam V., Bron E., Cazaux S., Dulieu F., Gry C., Guillard P., Habart E., et al., 2017, *MolAs*, 9, 1.
 Watanabe N., Kouchi A., 2002, *ApJ*, 571, L173.
 Wong B. A., Collinge G., Hensley A. J. R., Wang Y., McEwen J.-S., 2019, *PrSS*, 94, 100538.
 Yates J. T., Thiel P. A., Weinberg W. H., 1979, *SurSc*, 84, 427.

Zhao G., Chang Q., Zhang X., Quan D., Zhang Y., Li X.-H., 2022, *MNRAS*, 512, 3137.

This paper has been typeset from a $\text{\TeX}/\text{\LaTeX}$ file prepared by the author.